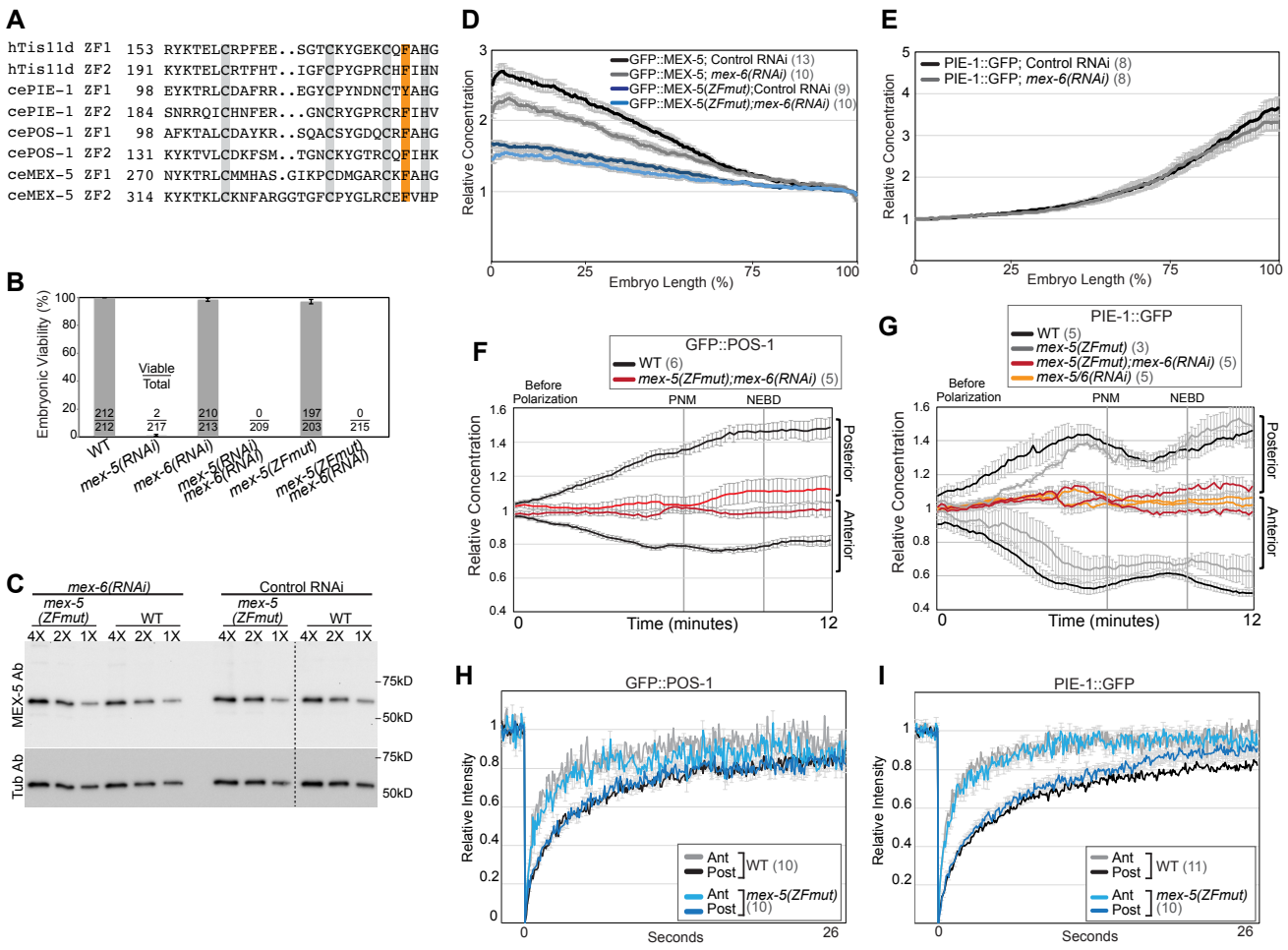

Figure S1. Characterization of mex-5(ZFmut) and mex-6(RNAi) embryos. Related to Figure 1.

(A) Alignment of the first and second CCCH zinc finger domains of human Tis11d and C. elegans PIE-1, POS-1 and MEX-5. The residues mutated to generate MEX-5(ZFmut), POS-1(ZFmut) and PIE-1(ZFmut) are highlighted in orange. The CCCH residues are highlighted in grey. **(B)** Viability of the embryos of the indicated genotype. The total number of embryos hatched (Viable) and laid (Total) are indicated. **(C)** Western blot of whole worm lysates from wild-type and mex-5(ZFmut) homozygous worms treated with control RNAi or mex-6(RNAi). Blots were probed with a MEX-5 antibody (top panel) and with a Tubulin antibody as a loading control (bottom panel). 4X, 2X and 1X lysate volumes were loaded for each sample. Stippled line indicates regions of the blot that were cropped together. **(D)** Relative concentration of GFP::MEX-5 and GFP::MEX-5(ZFmut) in wild-type and mex-6(RNAi) embryos. Normalized to the posterior. **(E)** Relative concentration of PIE-1::GFP in wild-type and mex-6(RNAi) embryos. Normalized to the anterior. **(F, G)** Average GFP::POS-1 and PIE-1::GFP concentration in the anterior and posterior cytoplasm from the completion of meiosis to just prior to cytokinesis in embryos of the indicated genotype. **(H, I)** FRAP curves for GFP::POS-1 and PIE-1::GFP in the anterior and posterior cytoplasm of wild-type and mex-5(zfmut) mutant embryos.

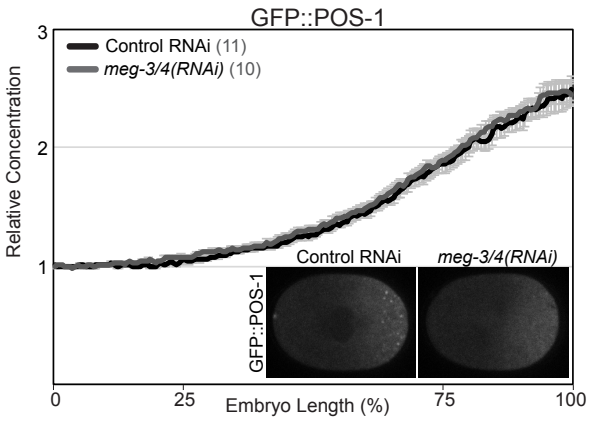

Figure S2. MEG-3/4 are not required for GFP::POS-1 segregation. Related to Figure 1.

Relative concentration of GFP::POS-1 along the A/P axis in control RNAi and meg-3/4(RNAi) embryos. Inset: Images of control RNAi and meg-3/4(RNAi) embryos expressing GFP::POS-1.

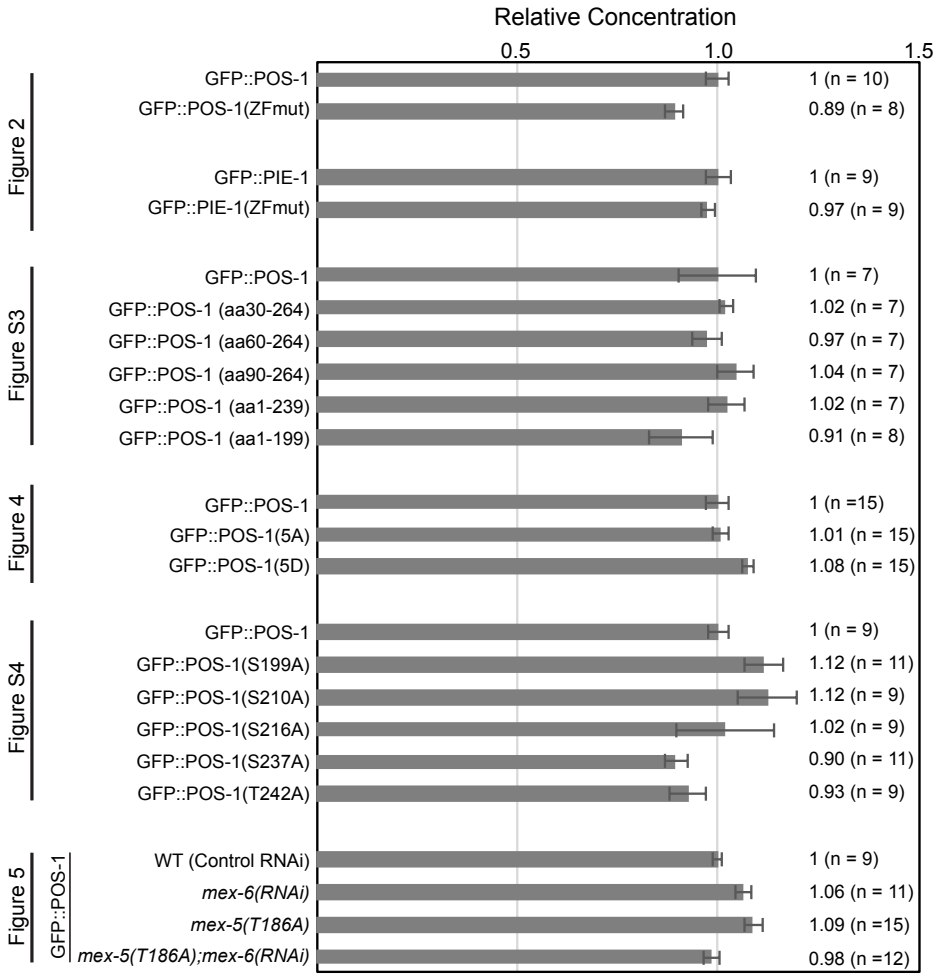

Figure S3. GFP transgene expression levels. Related to Figures 2, 4 and 5

.

The average GFP fluorescence was measured from images taken at the cell midplane of embryos at NEBD. The same images were used to quantify concentration gradients along the A/P axis in the indicated Figure panels. For each group of embryos in a panel, the intensity was normalized to the wild-type control. The number of embryos analyzed and the average intensity are presented to the right.

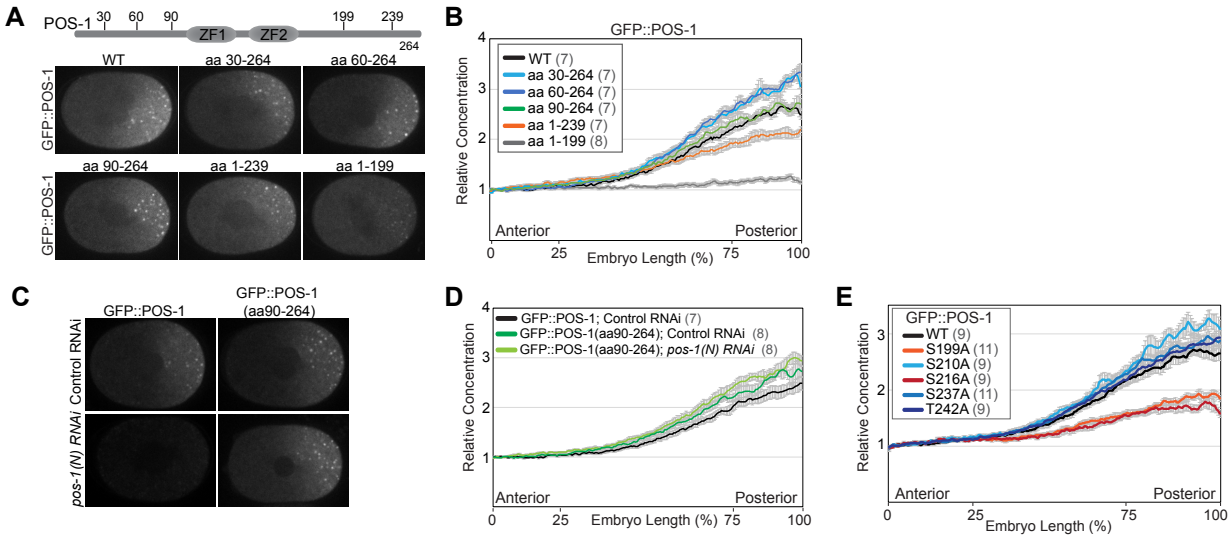

Figure S4. Structure/function analysis of GFP::POS-1. Related to Figure 3.

(A) Schematic of the POS-1 N-terminal and C-terminal truncations and images of embryos expressing the indicated GFP::POS-1 alleles. **(B)** Average intensity of GFP::POS-1 along the A/P axis comparing the wild-type and truncation alleles. Note that GFP::POS-1(1-199) is uniformly localized. **(C)** Images of GFP::POS-1 and GFP::POS-1 (aa90-264) in embryos treated with control RNAi or pos-1(N) RNAi, which targets the portion of POS-1 encoding residues 1-89. pos-1(N) RNAi efficiently depletes full length GFP::POS-1, but does not affect the GFP::POS-1(aa90-264) gradient. **(D)** Average intensity of the indicated GFP transgene in control RNAi and pos-1(N) RNAi embryos. **(E)** Average intensity of GFP::POS-1 along the A/P axis comparing the wild-type and the indicated mutant alleles.

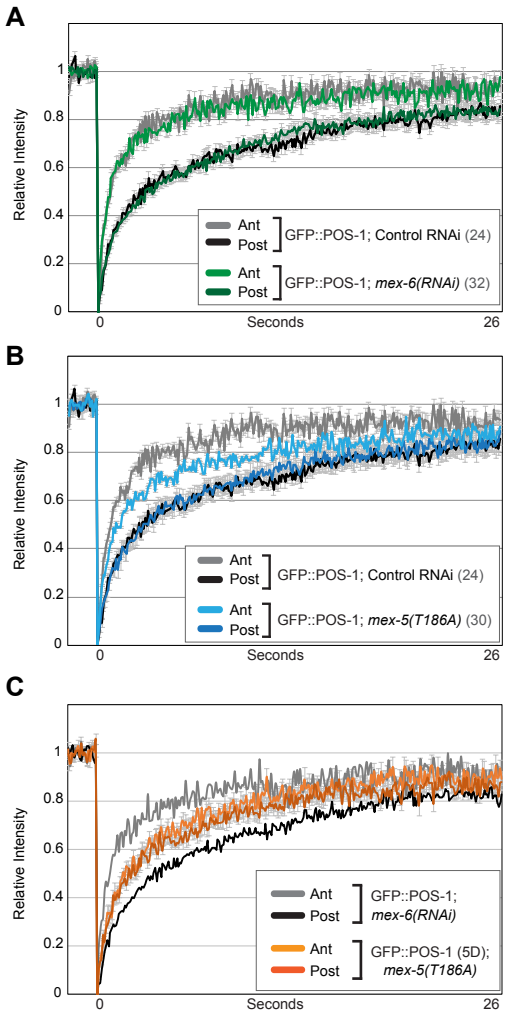

Figure S5. GFP::POS-1 dynamics in mex-6(RNAi) and mex-5(T186A) embryos. Related to Figure 5.

FRAP curves for GFP::POS-1 and GFP::POS-1(S5D) in **(A)** mex-6(RNAi) and **(B, C)** mex-5(T186A) embryos.

	Genotype	n	Anterior $t_{1/2}$, seconds (SEM)	Posterior $t_{1/2}$, seconds (SEM)	Anterior % recovery (SEM)	Posterior % recovery (SEM)
Figures 1 and S1	GFP::POS-1; control RNAi	10	1.34 (0.22)	3.32 (0.20)	92.0 (2.9)	82.6 (1.7)
	GFP::POS-1 *mex-5/6(RNAi)*	11	3.57 (0.38)	3.60 (0.24)	88.2 (1.3)	82.6 (1.9)
	GFP::POS-1 *mex-5(ZFmut)*	10	1.48 (.16)	3.39 (.46)	86.8 (21)	83.4 (2.4)
	GFP::POS-1 *mex-5(ZFmut);mex-6(RNAi)*	10	3.36 (.37)	3.59 (.24)	85.5 (2.4)	84.2 (1.6)
	GFP::PIE-1; control RNAi	11	1.26 (.16)	3.98 (.45)	95.0 (1.4)	82.0 (2.3)
	GFP::PIE-1 *mex-5/6(RNAi)*	10	3.97 (.36)	5.02 (.61)	77.3 (3.7)	83.0 (3.0)
	GFP::PIE-1 *mex-5(ZFmut)*	10	1.64 (.38)	4.62 (.61)	95.6 (2.0)	92.0 (4.8)
	GFP::PIE-1 *mex-5(ZFmut);mex-6(RNAi)*	10	5.45 (.65)	4.71 (.33)	82.2 (3.7)	81.9 (2.3)
Figure 2	GFP::POS-1; control RNAi	10	1.34 (0.22)	3.32 (0.20)	92.0 (2.9)	82.6 (1.7)
	GFP::POS-1(ZFmut); control RNAi	10	1.55 (.10)	1.69 (.24)	95.3 (1.6)	88.7 (2.3)
	GFP::POS-1; *mex-5/6(RNAi)*	11	3.57 (.38)	3.61 (.24)	88.2 (1.3)	82.6 (1.9)
	GFP::POS-1(ZFmut); *mex-5/6(RNAi)*	11	1.47 (.11)	1.23 (.13)	91.9 (1.8)	89.3 (1.7)
	GFP::PIE-1; control RNAi	10	1.13 (.13)	6.68 (.69)	89.2 (1.2)	82.9 (4.2)
	GFP::PIE-1(ZFmut); control RNAi	10	0.81 (.07)	3.11 (.19)	95.2 (1.5)	80.1 (1.8)
	GFP::PIE-1; *mex-5/6(RNAi)*	10	6.17 (.43)	5.42 (.34)	78.1 (3.1)	70.3 (1.8)
	GFP::PIE-1(ZFmut); *mex-5/6(RNAi)*	10	3.87 (.27)	3.41 (.34)	84.4 (2.1)	80.3 (3.2)
Figures 3 and 4	GFP::POS-1 (Fig. 3)	10	1.83 (.20)	3.83 (.52)	90.6 (2.2)	80.8 (4.5)
	GFP::POS-1; *plk-1(RNAi)* (Fig. 3)	15	3.55 (.18)	3.77 (.25)	84.6 (1.8)	85.5 (3.3)
	GFP::POS-1	35	1.45 (.19)	3.79 (.30)	90.3 (1.5)	80.9 (1.4)
	GFP::POS-1(5A)	31	2.58 (.19)	4.50 (.93)	86.0 (1.6)	85.6 (3.8)
	GFP::POS-1(5D)	22	1.97 (.30)	2.3 (.33)	90.3 (2.8)	84.0 (2.1)
	GFP::POS-1; *mex-5/6(RNAi)*	10	3.8 (.22)	3.1 (.22)	85.7 (2.3)	81.2 (1.8)
	GFP::POS-1(5A); *mex-5/6(RNAi)*	12	3.3 (.29)	4.0 (.35)	80.9 (2.5)	83.2 (2.0)
	GFP::POS-1(5D); *mex-5/6(RNAi)*	13	2.3 (.17)	2.88 (.18)	87.4 (1.3)	89.8 (2.3)
	GFP::POS-1; *plk-1(RNAi)*	10	2.86 (.42)	3.00 (.48)	81.1 (2.4)	82.4 (3.4)
	GFP::POS-1(5A); *plk-1(RNAi)*	9	4.13 (.44)	3.16 (.42)	84.0 (2.7)	74.3 (2.6)
	GFP::POS-1(5D); *plk-1(RNAi)*	11	1.83 (.15)	2.4 (.25)	89.0 (2.0)	85.8 (1.8)
	GFP::POS-1; *par-1(RNAi)*	13	1.97 (.35)	1.6 (.17)	92.0 (2.2)	88.2 (1.8)
	GFP::POS-1(5A); *par-1(RNAi)*	11	3.56 (.36)	3.57 (.42)	94.1 (3.7)	87.7 (2.8)
	GFP::POS-1(5D); *par-1(RNAi)*	11	2.44 (.38)	1.91 (.19)	92.7 (2.7)	87.7 (1.9)
	GFP::POS-1; *mbk-2(RNAi)*	23	3.06 (.27)	3.69 (.41)	85.7 (2.7)	81.6 (4.5)
Figure 5 and S5	GFP::POS-1; control RNAi	24	1.60 (.17)	4.77 (.60)	91.9 (1.5)	84.4 (3.2)
	GFP::POS-1; *mex-6(RNAi)*	32	1.64 (.12)	4.95 (.71)	89.7 (.87)	88.1 (4.1)
	GFP::POS-1; *mex-5(T186A);mex-6(RNAi)*	30	4.06 (.24)	3.81 (.15)	78.3 (1.7)	79.1 (1.5)
	GFP::POS-1(5D); *mex-5(T186A);mex-6(RNAi)*	48	3.15 (.16)	3.30 (.21)	85.4 (1.0)	86.9 (1.3)
	GFP::POS-1; *mex-5(T186A)*	30	2.68 (.26)	4.34 (.56)	104.3 (4.5)	84.8 (2.3)
	GFP::POS-1(5D); *mex-5(T186A)*	27	2.85 (.26)	3.05 (.27)	90.5 (1.5)	85.3 (1.6)
	PLK-1::GFP; control RNAi	11	2.79 (0.17)	1.95 (0.32)	92.7 (1.1)	91.0 (1.5)
	PLK-1::GFP; *mex-5/6(RNAi)*	11	1.66 (0.18)	2.13 (0.21)	93.3 (1.4)	94.5 (1.4)

Table S1. FRAP measurements. Related to Figures 1 – 5.

Quantification of the mean half-time of recovery ($t_{1/2}$) and percent recovery for FRAP experiments. The same measurements for GFP::POS-1 and GFP::PIE-1 treated with control RNAi are presented in both Figure 1 and 2. Control RNAi was performed using empty L4440 vector.